Hyperfine Effects on Associative Ionization of Ultracold Sodium

M. E. Wagshul, K. Helmerson, P. D. Lett, S. L. Rolston, and W. D. Phillips
Atomic Physics Division, National Institute of Standards and Technology, Gaithersburg, Maryland 20899

R. Heather and P. S. Julienne
Molecular Physics Division, National Institute of Standards and Technology, Gaithersburg, Maryland 20899
(Received 11 January 1993)

We observe a new resonance structure in the associative ionization spectrum of laser-cooled sodium due to the collision of two atoms in different ground hyperfine states. This associative ionization is due to doubly resonant excitation at moderate internuclear separation through intermediate molecular states. Substructure within this resonance is evidence for the role of molecular bound states in this process. We present calculations modeling the effect of ground-state hyperfine structure, the importance of which was unanticipated in earlier theoretical studies.

PACS numbers: 34.50.Rk, 32.80.Pj, 34.50.Gb

We have performed new single-color experiments that explore the associative ionization (AI) reaction ($Na+Na+2h\nu \rightarrow \cdots \rightarrow Na_2^+ + e^-$) as a function of laser frequency in ultracold sodium. The experiments reveal an important role for hyperfine structure in this reaction. Sodium AI is a model system for understanding excited-state collision processes and the ease of product-ion detection makes it an attractive subject for experimental study [1–11]. The collision energies in our experiments are much smaller than the ground-state hyperfine splitting, and allow us to investigate features related to this splitting, which would be extremely difficult to see at higher collision energies. These experiments represent a new kind of spectroscopy of Na_2, i.e., photoassociative ionization spectroscopy, where we are able to study weakly bound molecular intermediate states by looking at the AI spectrum.

The role of ground-state hyperfine structure was unanticipated before these experiments, but is easily explained. Two colliding atoms are resonantly excited by a single color only at long range. At the low velocity of ultracold collisions the doubly excited quasimolecule is likely to undergo spontaneous emission before reaching the small internuclear distance of the Na_2^+ curve crossing where AI takes place [2,6,11–14]. The hyperfine structure allows one-color excitation to be doubly resonant at a reduced internuclear distance, leading to an increased probability for AI. Resonances in the AI rate as a function of laser frequency indicate the role of bound intermediate states of the Na_2 molecule.

Previous experiments have investigated AI under ultracold (≤ 1 mK) conditions [3,4,10,11] with the exciting laser also providing confinement and/or cooling for the reacting atoms. The tuning range to the red of the trapping transition ($3^2S_{1/2}$, $F=2 \rightarrow 3^2P_{3/2}$, $F'=3$) was therefore limited and any investigation of the blue of this frequency was impossible. Using a separate excitation laser we are able to examine, in particular, the region between the $F=2 \rightarrow F'=3$ and the $F=1 \rightarrow F'=2$ transitions in atomic sodium. By separating the trapping and AI excitation processes in time we are able to explore this region with single-color excitation, where we find the hyperfine-induced, doubly resonant associative ionization.

These experiments were performed using a magneto-optical trap (MOT) [15] continuously loaded from a Zeeman-cooled atomic beam [16]. This trap supplies a relatively large number of atoms ($\sim 10^8$) at high density ($\sim 10^{10}$ cm^{-3}) and low temperature (≤ 500 μK). The trapping laser (~ 35 mW/cm^2 per beam) is tuned one linewidth (10 MHz) below the $F=2 \rightarrow F'=3$ resonance and has $\sim 10\%$ sidebands, one of which optically pumps atoms out of the $F=1$ back into the $F=2$ ground states. The trapping laser is alternated with a second, AI laser, and ion counters are gated open during the trap-off intervals to obtain the single-color AI rate. The switching is performed by acousto-optic modulators with a $\sim 50\%$ duty factor and MOT/AI intervals of 2–100 μs. The AI laser can be easily tuned over a broad range and, when retroreflected (total intensity ~ 3 W/cm^2) in a polarization configuration resembling that of the MOT trapping lasers, does little to perturb the confinement of the atoms except when tuned very near the atomic transition frequencies. Additional counters are gated open only during the MOT intervals; these counts are recorded simultaneously and used as a monitor of the effect of the AI laser on the number and density of atoms in the trap.

A spectrum obtained in this way is shown in Fig. 1. The positions of the $F=2 \rightarrow F'=3$ and the $F=1 \rightarrow F'=2$ transitions are indicated. A broad resonance structure rises sharply from a threshold approximately halfway between them and extends to the blue toward the $F=1$ transition. We have verified that this represents a two-photon process; the height of the peak is proportional to the square of the AI laser intensity over the range 0.05 to 1.5 W/cm^2 and for short enough AI counting intervals. For intervals that are too long optical pumping becomes a complicating factor, as discussed below.

The general features of Fig. 1 can be understood, in a semiclassical picture ignoring the small P-state hyperfine structure, by referring to Fig. 2. Simplified molecular po-

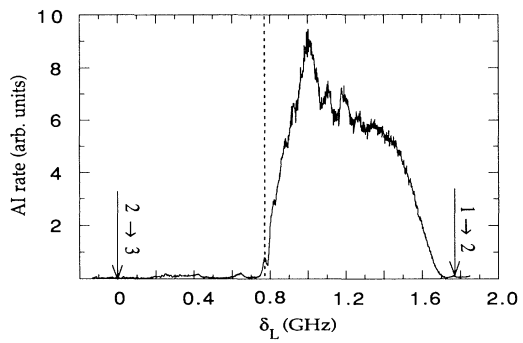

FIG. 1. Ion counts as a function of AI laser detuning, δ_L. The positions of the $F=2 \rightarrow F'=3$ and $F=1 \rightarrow F'=2$ atomic transitions are indicated. The laser intensity was ~ 3 W/cm^2. The dashed line indicates the predicted threshold discussed in the text.

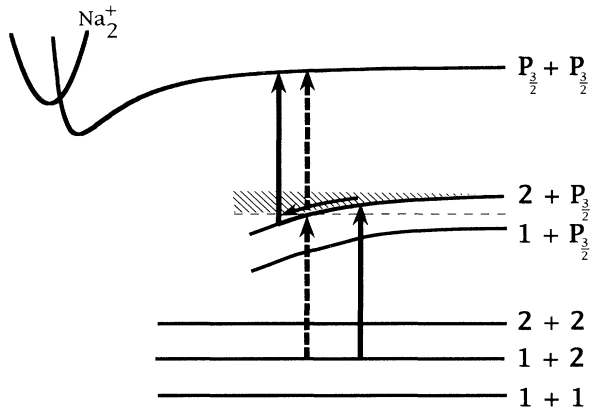

FIG. 2. Simplified schematic of the molecular potential curves. The atomic states that asymptotically correlate to the molecular potentials are labeled at the right. The $F=1$ and $F=2$ ground hyperfine states are indicated by 1 and 2.

tential curves are labeled by the asymptotic (large internuclear separation) atomic state labels. At large internuclear distances two $F=2$ atoms can be excited to the $P+P$ potential by two photons at the $F=2 \rightarrow P$ atomic resonance frequency. In this molecular picture this represents a doubly resonant two-photon excitation. Given the extremely slow approach velocity in an ultracold collision, however, the AI rate is reduced due to the lack of survival in the excited state. Similarly, two $F=1$ atoms can be doubly resonantly excited at long range by a single laser frequency but survival in the excited $P+P$ state to AI is unlikely.

When atoms in different ground hyperfine states collide (on the potential labeled $1+2$), the double resonance condition cannot be satisfied at long range. The photon energy required for two-photon $P+P$ excitation falls halfway between the potentials labeled $1+P$ and $2+P$, as indicated by the dashed line. At $\sim 400 a_0$, however, the attractive $2+P$ potential crosses this line and the transition is doubly resonant, as indicated by the dashed arrows. Excitation at this distance reduces the spontaneous emission losses, increasing the probability of AI. In this simplified model, light to the red of this frequency cannot provide enough energy to reach the $P+P$ potential from the $1+2$ state. This results in an energy threshold for AI. Light to the blue of this frequency can provide a resonant excitation to the $2+P$ state at increasing internuclear distances. Semiclassically, the atoms then accelerate on the $2+P$ potential and can be resonantly excited to the $P+P$ state at closer range (solid arrows), leaving the atoms with some additional kinetic energy. When the light is bluer than the asymptotic separation of the $1+2$ and $2+P$ potentials the intermediate resonance condition is lost. The allowed energy range for doubly resonant excitation is indicated by the shaded area in Fig. 2.

Further support for this interpretation of the AI mechanism was found using two excitation frequencies. When we initially observed AI, with the AI laser on at the same time as the MOT laser, we found a complicated spectrum with strong AI immediately blue of the $F=2$ resonance, decreasing towards the $F=1$ resonance, with a similar large rate blue of $F=1$ as well. The desire to simplify this complicated situation led us to the alternated single-color experiment described above. We also performed an alternated two-color experiment. With one laser tuned to $1 \rightarrow P$ we see a peak in the AI rate as a second laser is scanned immediately blue of $2 \rightarrow P$. This can be explained by referring to Fig. 2: In this case we excite from the $1+2$ ground state to the $2+P$ intermediate state at the relatively small internuclear separation that brings this intermediate state into resonance with the laser tuned near $2 \rightarrow P$. Then the additional $1 \rightarrow P$ photon is also exactly resonant to the doubly excited state. Similarly, addition of light tuned to the $2 \rightarrow P$ resonance produces enhancement to the blue of the $1 \rightarrow P$ transition. "Two-color" experiments using the MOT laser for the second color are, in fact, more than two color and complicated since the MOT, tuned near $2 \rightarrow P$, has at least one additional repumper frequency near $1 \rightarrow P$. In our case this leads to at least five broad resonances as the laser is tuned. We will restrict our further discussions to single-color measurements.

Both the magnitude and shape of the single-color resonance structure in Fig. 1 are affected by optical pumping. The AI rate for the process described above depends on the product of the $F=1$ and $F=2$ ground-state population densities n_1 and n_2, respectively, and this product depends strongly on optical pumping effects. We can increase the initial population in the $F=1$ state by turning off the repumping sidebands on the laser during the last few microseconds of the MOT trapping interval. The AI rate has a maximum as a function of this optical pumping time, which we interpret as occurring when the $F=1$ and

$F=2$ ground-state populations are equal. The envelope of the spectrum of Fig. 1 is affected by optical pumping because near the $F=1$ resonance the atoms are optically pumped mostly into the $F=2$ state and the AI process, as described above, is suppressed. We observe less suppression for lower laser intensity where optical pumping is less rapid. Furthermore, we have operated the experiment with the AI laser on for ~ 10 μs intervals but with the ion counter gates open only for ~ 2 μs. As the gate window is shifted from the beginning of this period to the end we find that the AI near the $1 \rightarrow P$ transition is suppressed, as expected from optical pumping. An additional factor affecting the envelope is that as the AI laser approaches the atomic resonance frequency, the radiation pressure force and extra heating due to this laser can also lead to large perturbations of the temperature and density of the MOT. Normally such perturbations are restricted to a small frequency interval near the resonances.

We did not measure the absolute size of the AI rate coefficiently directly. It was determined, however, that using the typical operating parameters indicated above to within a factor of 2, the total rate of ion production during the MOT interval was equal to the peak ion production rate during the AI interval under optical pumping conditions where we believe the ground hyperfine state populations to be equal. Using the recently measured MOT AI rate coefficients [10], which are in agreement with the low intensity measurements of Ref. [4], we can estimate a rate coefficient for the $1+2$ process to be $K_{1+2} \sim 10^{-13}$ cm^3/s, where the rate of production of Na_2^+ ions per unit volume is $2n_1n_2K_{1+2}$.

An extremely interesting feature of the broad resonance in Fig. 1 is its small scale structure. This substructure consists of a number of resonances, the narrowest of which occur on its sharply rising edge. The positions of these resonances appear to be unaffected by optical pumping or changes of laser intensity. We ascribe the substructure to molecular bound states. In order to describe such substructure we need a more sophisticated model than the semiclassical one described above.

Therefore, we have calculated the rate coefficient as a function of frequency using a quantum close-coupling model similar to that of Ref. [6]. The original model was modified to simulate the effect of ground-state hyperfine structure by lowering the ground-state potential by the atomic ground-state hyperfine splitting, Δ_{hf}, to correspond to $1+2$ collisions. According to Ref. [6] the doubly excited 1_u state of Na_2 dominates AI [7,8] at these temperatures, so, given the dipole selection rules, we assume that atoms come together only on the $^3\Sigma^+_u$ molecular ground-state potential. The atoms are excited to intermediate 0_g^- and 1_g molecular states at internuclear separations, $R > 360a_0$, and in a second step, to the doubly excited 1_u state which autoionizes at small R and which correlates at large R with two separated $^2P_{3/2}$-state atoms. The calculated photoassociative ionization spectrum is shown in Fig. 3.

The location of the substructure is dominated by the energies of the 0_g^- vibrational levels, rather than the 1_g levels, because the $0_g^- \rightarrow 1_u$ radiative coupling is larger than the $1_g \rightarrow 1_u$ coupling. The calculated substructure is simpler and more distinct than that seen experimentally because the model neglects the molecular aspects of hyperfine structure as well as excited P-state hyperfine structure. The calculated spectrum was artificially broadened to simulate the effects of excited-state radiative decay and hyperfine-induced predissociation to the $1+P$ separated atom state. We estimate the broadening to be 50 MHz. The broadening was approximated by convolving with a Lorentzian of this width. This produces an unphysical broadening of the threshold in Fig. 3.

The calculation shows that significant AI occurs only in the detuning range from a point halfway between the $2 \rightarrow P$ and $1 \rightarrow P$ resonance frequencies, up to the $1 \rightarrow P$ frequency. The transition is free bound free and energetically allowed only when the laser detuning $\delta_L > \Delta_{hf}/2 = 886$ MHz ($\delta_L = 0$ at the $F=2 \rightarrow F'=3$ resonance). The expected experimental threshold (dashed line in Fig. 1) is lower by 110 MHz, the splitting between the excited $F'=3$ and $F'=0$ states. (Note that the atomic hyperfine selection rules do not apply in the molecular environment.) Experimentally we observe the sharp rise to begin within ~ 10 MHz of this predicted threshold. The calculation, in the absence of broadening, gives a sharp onset to the ionization signal at threshold and substructure due to the bound states of the 0_g^- and $1g$ potentials. A proper theoretical treatment would require taking into account the details of the molecular hyperfine structure, its variation with R, and its effect on radiative transition probabilities, so our results are only qualitative. As the laser frequency increases toward the $1 \rightarrow P$ resonance, the density of vibrational and rotational states becomes large enough that the bound-state structure is blended into a pseudocontinuum. Once the laser is blue of the $1 \rightarrow P$ resonance, the spectral density due to $1+2$ collisions becomes negligible because of the Franck-Condon principle. The first transition no longer has a real Condon point

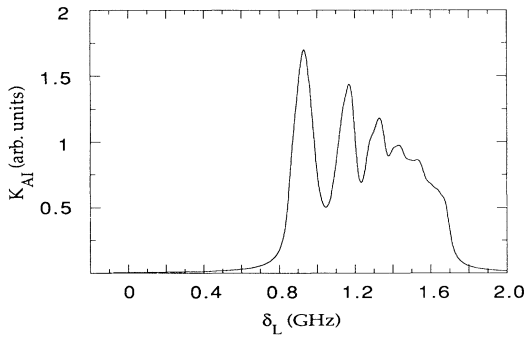

FIG. 3. Theoretical calculation of the AI rate coefficient using the model system discussed in the text. A laser intensity of 1 W/cm^2 was used in the calculation.

where the photon energy matches the difference between the ground and intermediate molecular potentials; thus the Franck-Condon overlap matrix elements become negligibly small.

Comparing Fig. 3 to Fig. 1, we find that our simple model correctly predicts a number of qualitative features: the steep rise in the ionization rate near the observed threshold frequency, the existence of AI from the threshold to the $F=1$ resonance, and the existence of substructure. Our model does, however, overestimate the actual rate by over an order of magnitude. It is clear that a complete treatment of hyperfine structure in the molecular environment will be necessary to make a quantitative comparison between theory and experiment; such a treatment is in progress.

The AI reaction, as described here, is a molecular multistep process that is in many ways extremely different from the reaction at high temperatures. This has led to the adoption of the term photoassociative ionization to refer to the process, in order to emphasize the central role of the complicated photoexcitation during the reaction at these energies [6,10,14].

Finally we note that there are weak resonances in Fig. 1 in the region that is energetically forbidden in the $1+2$ process described above. We believe that the sources of these resonances are free-bound-bound transitions [6], from collisions of two atoms in the $F=1$ state. Evidence of free-bound-bound transitions was seen in Ref. [4], but interpretation is difficult due to the high laser intensities used in that work. We hope to explore these weak resonances and features that appear to the red of the $2\rightarrow P$ transition in future publications. Our preliminary results indicate that there is a rich field of two-color experiments to be explored as well. We intend to do such experiments with independent frequency control of the two lasers, to allow identification of the individual levels in the intermediate states that contribute to AI. Pure long-range states [17] of the 0_g^- potential have never been directly observed. In the future, we hope to capitalize on the extremely good energy resolution afforded by our ultracold atoms to probe such tenuously bound molecules.

We thank T. J. McIlrath for providing key insights into the role of hyperfine structure. This work was partially supported by the U.S. Office of Naval Research. K.H. and M.E.W. are NRC postdoctoral fellows.

[1] J. Weiner, F. Masnou-Seeuws, and A. Giusti-Suzor, Adv. At. Mol. Phys. **26**, 209 (1989), and references therein.
[2] P. Julienne, Phys. Rev. Lett. **61**, 698 (1988).
[3] P. Gould, P. Lett, P. Julienne, W. Phillips, H. Thorsheim, and J. Weiner, Phys. Rev. Lett. **60**, 788 (1988).
[4] P. Lett, P. Jessen, W. Phillips, S. Rolston, C. Westbrook, and P. Gould, Phys. Rev. Lett. **67**, 2139 (1991).
[5] A. Gallagher, Phys. Rev. A **44**, 4249 (1991).
[6] P. Julienne and R. Heather, Phys. Rev. Lett. **67**, 2135 (1991); R. Heather and P. Julienne, Phys. Rev. A **47**, 1887 (1993).
[7] O. Dulieu, A. Giusti-Suzor, and F. Masnou-Seeuws, J. Phys. B **24**, 4391 (1991).
[8] A. Henriet, F. Masnou-Seeuws, and O. Dulieu, Z. Phys. D **18**, 287 (1991).
[9] H. Meijer, S. Schol, H. Dengel, M. Muller, M. Ruf, and H. Hotop, J. Phys. B **24**, 3621 (1991).
[10] V. Bagnato, L. Marcassa, Y. Wang, J. Weiner, P. Julienne, and Y. Band (to be published).
[11] P. Gould, P. Lett, R. Watts, C. Westbrook, P. Julienne, W. Phillips, H. Throsheim, and J. Weiner, in *Atomic Physics 11* (World Scientific, Teaneck, NJ, 1989), p. 215.
[12] P. Julienne and J. Vigue, Phys. Rev. A **44**, 4464 (1991).
[13] A. Gallagher and D. Pritchard, Phys. Rev. Lett. **63**, 957 (1989).
[14] Y. Band and P. Julienne (to be published).
[15] E. Raab, M. Prentiss, A. Cable, S. Chu, and D. Pritchard, Phys. Rev. Lett. **59**, 2631 (1987).
[16] W. Phillips, J. Prodan, and H. Metcalf, J. Opt. Soc. Am. B **2**, 1751 (1985).
[17] W. Stwalley, Y.-H. Uang, and G. Pichler, Phys. Rev. Lett. **41**, 1164 (1978).